Cancer Gene Therapy (2016) 23, 287–294

www.nature.com/cgt

ORIGINAL ARTICLE

Loss of asparagine synthetase suppresses the growth of human lung cancer cells by arresting cell cycle at G0/G1 phase

Yi Xu[1,3], Fanzhen Lv[2,3], Xunxia Zhu[2], Yun Wu[2] and Xiaoyong Shen[2]

The aim of this research is to determine the role of human asparagine synthetase (*ASNS*) in human lung cancer. In the present study, immunohistochemical staining and the Oncomine database mining showed that the expression of *ASNS* gene was higher in lung cancer tissues than that in the normal tissues by. In addition, western blot assay showed that *ASNS* was elevated in lung cancer A549 and 95D cell lines as compared with that in H1299 and H460 cells. Therefore, A549 and 95D cells were chosen for subsequent MTT and colony formation assay. It was found that knockdown of *ASNS* inhibited the growth and colony formation abilities of A549 and 95D cells. Flow cytometry showed that *ASNS* silencing arrested cell cycle progression at G0/G1 phase in A549 cells, probably through regulating the expression of cell cycle molecules such as CDK2 and Cyclin E1 as shown by quantitative real-time PCR. Taken together, our study indicates that *ASNS* may be an important target for lung cancer diagnosis and treatment.

Cancer Gene Therapy (2016) **23,** 287–294; doi:10.1038/cgt.2016.28; published online 22 July 2016

INTRODUCTION

Lung cancer is the most common malignant tumor in the respiratory system and the leading cause of cancer-related death worldwide, accounting for more than 27% of all cancer deaths.[1] The 5-year relative survival of lung cancer is about 18% at present because most patients are diagnosed at an advanced stage, in whom 5-year survival is only about 4%.[1] According to the latest cancer statistics in China, new lung cancer patients have exceeded 700 000 and more than 600 000 patients died of lung cancer in 2015.[2] Lung cancer poses a serious threat to human health but its exact pathogenesis remains exclusive. Therefore, improving early diagnosis and screening out new biomarkers and therapeutic targets have become an urgent task in the research and treatment of human lung cancer.

The asparagine synthetase gene (*ASNS*) encodes the enzyme involved in the synthesis of asparagine in an ATP-dependent manner.[3] It has been reported that the transcription process of *ASNS* gene is dependent on the nutritional status of cells[4] and enhanced by amino acid deprivation.[5] Early studies showed that *ASNS* overexpression was related to asparaginase resistance to human leukemic cells.[6] Further studies indicated that up-regulation of *ASNS* expression could suppress cell apoptosis induced by glucose deprivation and cisplatin in pancreatic cancer.[7] In addition, *ASNS* was considered to be a fatidic indicator of L-asparaginase activity in ovarian cancer [8,9] and hepatocellular carcinoma cells.[10] Similarly, *ASNS* expression was found to be increased in castration-resistant prostate cancer, and asparagine depletion by using *ASNS* inhibitors could be a novel therapy for this disease.[11] However, to the best of our knowledge, the expression regulation and subsequent functional roles of *ASNS* in human lung cancer remain unknown. It is therefore warrantable to investigate the biological function of *ASNS* in human lung cancer.

In this study, we identified *ASNS* gene as a supposed oncogene in lung cancer cells by lentivirus shRNA library-based screening. To further study the function of *ASNS*, we compared the expression level of *ASNS* in normal and lung cancer tissues by using data mining of Oncomine database and immunohistochemical (IHC). Meanwhile, the effect of *ASNS* silencing in lung cancer cells and the possible mechanism underlying this effect were also studied.

MATERIALS AND METHODS

Oncomine database

To determine the clinical significance of *ASNS* expression in lung cancer, the online Oncomine database (www.onocomine.org) was used. First, filter combination was applied to show corresponding datasets so as to know the differences in *ASNS* expression between lung cancer and normal tissues. The Data Type was defined as mRNA, and the analysis type was cancer vs normal analysis. Each dataset revealed by the filters was analyzed separately. Differences in *ASNS* expression between different types of lung cancer and normal tissues were compared by using four datasets including Beer Lung,[12] Hou Lung,[13] Selamat Lung[14] and Stearman Lung.[15] The log-transformed and normalized expression values of *ASNS* were abstracted, analyzed and read from the scatterplot.

Clinical specimens and IHC assay

All the clinical specimens for IHC analysis were collected from the Department of Thoracic Surgery of Huadong Hospital affiliated to Fudan University (Shanghai, China). This study was approved by the Ethics Committee of the said hospital, and written informed consent was obtained from each subject in line with the Helsinki Declaration.

After deparaffinization and rehydration, 10 mM citrate buffer (pH 7.0) was used to microwave antigen retrieval. Subsequently, each specimen was incubated with blocking solution (BS) for 10 min and rabbit anti-ASNS antibody (14681-AP; Proteintech Group Inc., Chicago, IL, USA) with 100-fold dilution overnight at 4 °C and then stained using Histostain-Plus 3rd Gen

[1]Department of Respiration, The Affiliated Huadong Hospital of Fudan University, Shanghai, China and [2]Department of Thoracic Surgery, The Affiliated Huadong Hospital of Fudan University, Shanghai, China. Correspondence: Dr X Shen, Department of Thoracic Surgery, The Affiliated Huadong Hospital of Fudan University, No. 221 West Yan-an Road, Shanghai 200040, China.
E-mail: shenxiaoyong2014@163.com
[3]Fanzhen Lv and Yi Xu contributed equally to this study and should be regarded as co-first authors.
Received 8 April 2016; revised 5 June 2016; accepted 7 June 2016; published online 22 July 2016

IHC Detection Kit (Invitrogen, Carlsbad, CA, USA) according to the manufacturer's directions. The score of the proportion of positive tumor cells in the tissues was defined as 0: 0–5%; 1: 6–20%; 2: 21–60%; 3: 61–100%, and the score of the mean intensity of positive tumor cells in the tumor tissues was 0: negative; 1: weak; 2: moderate; 3: strong. The final IHC score was calculated as the addition product of the above two independent scores (0: negative; 1: weak positive; 2 ~ 4: positive; 5 ~ 6: strong positive) as described previously.[16,17]

Cell culture

Human lung cancer cell lines H1299, A549, H460 and 95D were obtained from the Cell Bank of Chinese Academy of Science (Shanghai, China), together with human embryonic kidney (HEK) 293 T cell line. HEK293T, A549, H460 and 95D cells were cultured in DMEM (Hyclone, Logan, UT, USA) supplemented with 10% fetal bovine serum (FBS, BioWest, Kansas City, MO, USA). Meanwhile, H1299 cells were cultured in RPMI-1640 medium (Hyclone, Logan, UT, USA) supplemented with 10% FBS, and then maintained at 37 °C humidified atmosphere of 5% CO_2.

Recombinant lentivirus construction and cell infection

To silence *ASNS* expression in lung cancer cell lines, the following short-hairpin RNA (shRNA) sequence was designed to against *ASNS* gene (NM_001673): 5′-GTGAACATTATGAAGTCCTTTCTCGAGAAAGGACTTCATAAT GTTCACTTTTT-3′, and the negative control shRNA was 5′-TTCTCCGAACGTG TCACGTCTCGAGACGTGACACGTTCGGAGAA-3′. The stem-loop-stem oligos were synthesized, annealed, and ligated into the *Nhe*I/*Pac*I-linearized pFH-L vector (Hollybio, Shanghai, China). The plasmid with correct insert was confirmed by DNA sequencing. The generated constructs were named as pFH-L-shASNS for targeting plasmid or pFH-L-shCon for negative controls. HEK293T cells were seeded into 10-cm dishes and cultured for 24 h to reach 70–80% confluence. Two hours before transfection, the medium was replaced with serum-free DMEM. Three plasmids including 10 μg pFH-L-

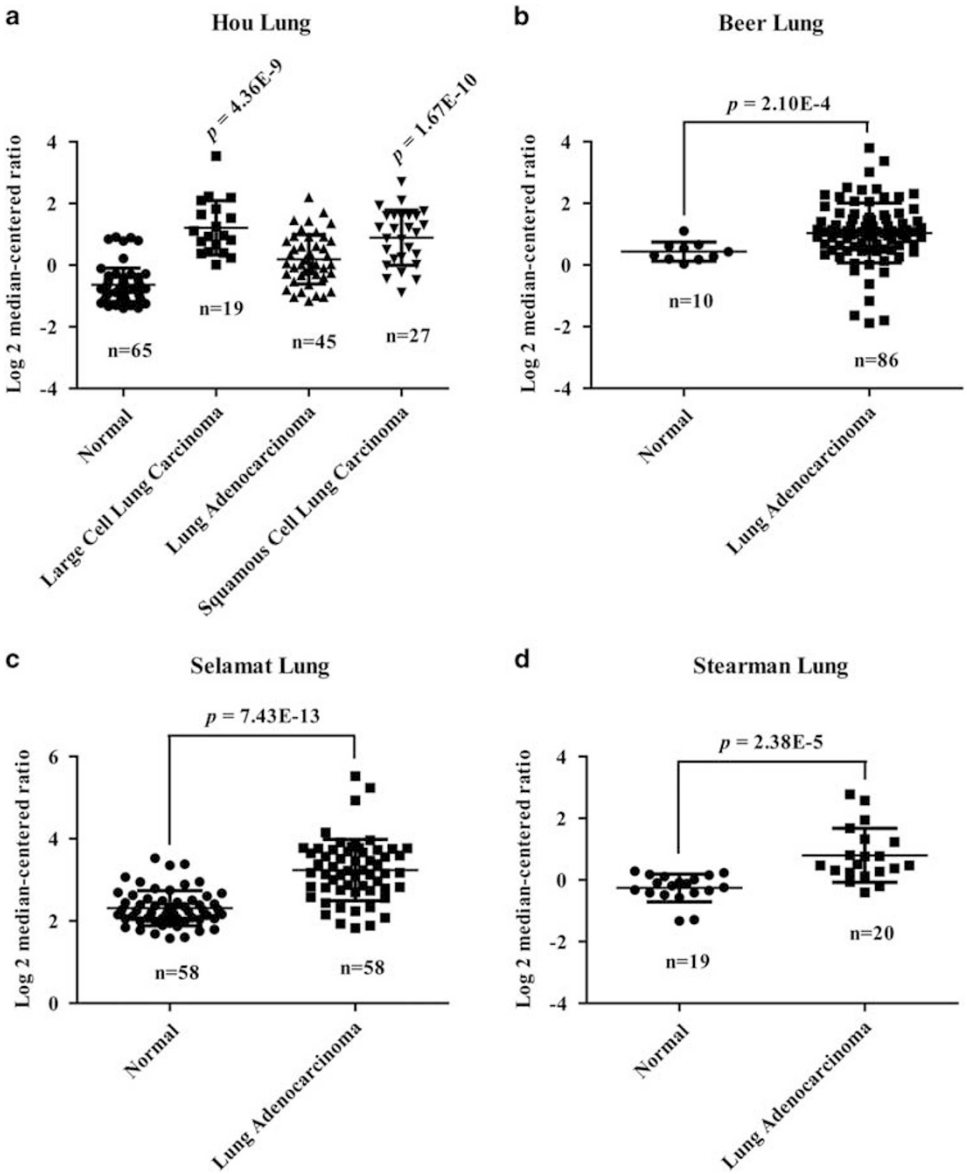

Figure 1. Overexpression of *ASNS* mRNA in lung cancer was revealed by the Oncomine database. (**a**) *ASNS* expression analysis in the normal lung, large cell lung carcinoma, lung adenocarcinoma and squamous cell lung carcinoma tissues as shown by the Hou Lung dataset. (**b–d**) Differential expression of *ASNS* in the normal and lung adenocarcinoma tissues as shown by the Beer Lung, Selamat Lung and Stearman Lung datasets, respectively. The total number of samples was shown under each category. The *P*-values were calculated using the two-tailed and unpaired Student's *t*-test.

shASNS (or pFH-L-shCon) expression plasmid, helper plasmids 7.5 μg pCMVΔR8.92 and 5 μg pVSVG-I were added to 950 μl serum-free DMEM and mixed with 50 μl Lipofectamine 2000 according to the manufacturer's instructions. HEK293T cells were co-cultured with the plasmid mixture for 6 h and then the medium was replaced with 10 ml DMEM medium supplemented with 10% FBS. Lentiviral particles were collected at 48 h after transfection. The viral titer was measured by end-point dilution assay by counting the number of green fluorescence protein (GFP)-positive cells under a fluorescent microscope (Epoch, BioTek, Winooski, VT, USA) after 96-h infection.

For lentivirus transduction, lung cancer A549 and 95D cells were cultured in 6-well plates at a density of 5×10^4 cells/well and inoculated with lentivirus containing *ASNS* shRNA (shASNS) or negative control shRNA (shCon) with a multiplicity of infection of 20 for A549 cells or 8 for 95D cells, respectively. The infection efficiency was assessed under the fluorescence microscope for GFP expression after 96-h infection.

Quantitative real-time PCR (qRT-PCR) analysis

Total RNA was extracted from A549 and 95D cells after 5-day lentivirus infection by using TRIzol reagent (Invitrogen, Carlsbad, CA, USA) according to the manufacturer's instruction and synthesized into complementary DNA (cDNA) by using M-MLV Reverse Transcriptase (Promega, Beijing, China). Real-time PCR reaction using a SYBR Premix Ex Taq (TaKaRa, Dalian, China) was run on a Bio-Rad Connect Real-Time PCR platform (Bio-Rad Laboratories Inc., Hercules, CA, USA). The thermal cycling program was as follows: initial denaturation for 1 min at 95 °C, followed by 40 cycles of denaturation for 5 s at 95 °C, extension for 20 s at 60 °C. The absorbance value was read at the extension stage. The relative gene expression level was calculated using $2^{-\Delta\Delta CT}$ analysis with normalization to the internal control β-actin. The primers used were as follows: ASNS (forward): 5′-TGCTT ACGCCCAGATTTTCT-3′; ASNS (reverse): 5′-AAAACGGAATGCATCTGGAC-3′; CDK2 (forward): 5′-TCCAGGATGTGACCAAGCC-3′; CDK2 (reverse): 5′-CTGAG TCCAAATAGCCCAAGG-3′; Cyclin E1 (forward): 5′-GGGTATCAGTGGTGCGA CAT-3′; Cyclin E1 (reverse): 5′-CCAGCAAATCCAAGCTGTCT-3′; β-actin (forward): 5′-GTGGACATCCGCAAAGAC-3′; β-actin (reverse): 5′-AAAGGGTG TAACGCAACTA-3′.

Table 1. ASNS immunohistochemical expressions in lung tissues

Tissues	*Total*	*Expression of ASNS*			P-*value*
		− *to* +	+	++	
Lung adenocarcinoma	49	3	16	30	0.003**
Normal	13	2	10	1	

When two groups were compared using the Pearson χ^2-test, there was a significant difference between them. $^{**}P < 0.01$.

Western blot analysis

Lung cancer cells were cultured and transfected with recombinant lentivirus shCon or shASNS for 6 days. The infected cells were lysed with ice-cold 2× sodium dodecyl sulfate (SDS) sample buffer (100 mM pH 6.8 Tris–HCl, 10 mM EDTA, 4% SDS, 10% glycine). Equal amounts of protein samples (30 μg) were separated by 10% SDS-polyacrylamide gel electrophoresis and electro-transferred to polyvinylidene difluoride membranes (Millipore, Bedford, MA, USA). The membranes were blocked in the sealing solution at room temperature for 1 h and probed with rabbit anti-ASNS antibody (1:3000 dilution, 14681-AP, Proteintech Group Inc., Chicago, IL, USA), and rabbit anti-GAPDH (1: 3000 dilution, 10494-AP, Proteintech Group Inc., Chicago, IL, USA) overnight at 4 °C. The membranes were then incubated with horseradish peroxidase-conjugated secondary antibody (1:5000 dilution, SC-2054, Santa Cruz, Dallas, TX, USA) at room temperature for 2 h and the target bands were visualized by using super ECL detection reagent (Applygen, Beijing, China) according to the instructions. GAPDH was used as the internal standard.

Cell proliferation assay

The MTT assay was carried out to evaluate the rate of cell proliferation. After 96- h infection, A549 and 95D cells were washed and re-cultured in the prepared 96-well plates at a density of 2500 cells per well for A549 or 2000 cells per well for 95D cells. Subsequently, MTT (20 μl, 5 mg/ml) was added into each well and incubated at 37 °C for 4 h. Then, 100 μl acidic isopropanol (10% SDS, 5% isopropanol, and 0.01M HCl) was added and incubated overnight at 37 °C. The optical density value was measured at 595 nm by using a microplate spectrophotometer (Epoch, BioTek, VT, USA).

Colony formation assay

After 96-h incubation, A549 and 95D cells were washed and re-cultured in the prepared 6-well plates at a density of 500 cells per well, and allowed to grow for 8 days to form natural colonies. The medium was replaced about every 2 days. Then cells were fixed in 4% paraformaldehyde for 10 min and stained with fresh crystal violet for 5 min at room temperature. The stained colonies were washed with ddH_2O and air-dried. Finally, cell colonies containing more than 50 cells were imaged and counted through a light/fluorescence microscope.

Flow cytometry analysis

The cell cycle distribution was determined by propidium iodide staining combined with flow cytometry analysis. In short, A549 cells were re-cultured at a density of 2×10^5 cells/dish in 6 cm dishes after lentivirus infection. After 40-h culture, cells were collected, washed in cold PBS and fixed in 70% ethanol overnight at 4 °C. The following day, cells were

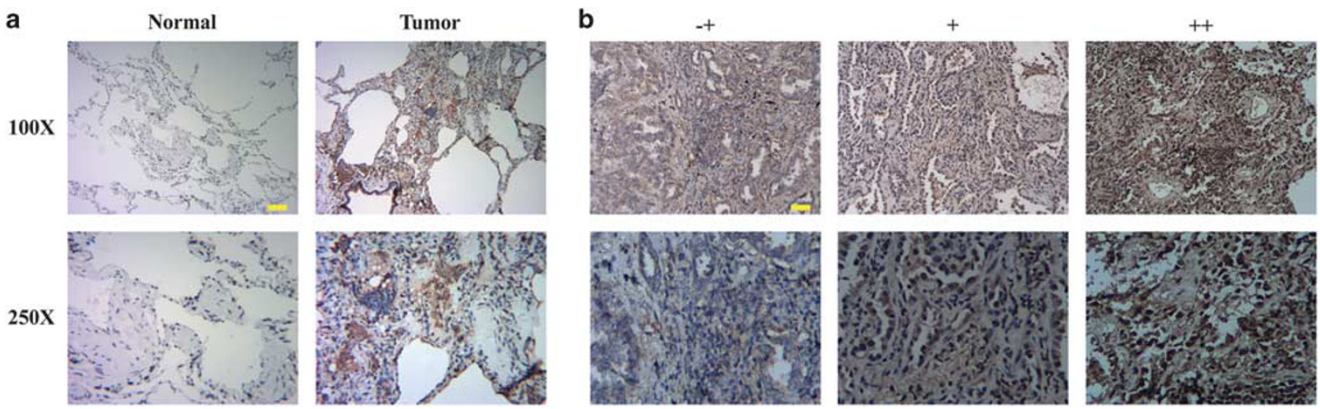

Figure 2. *ASNS* expression level in tissues was anlyzed by immunohistochemistry staining. (**a**) Representative immunohistochemical staining for *ASNS* in normal and tumor tissues. (**b**) The representative immunohistochemistry staining intensity of *ASNS* in tumor tissues. −, negtive; +, positive; ++, strong positive; 100× scales bar, 10 μm.

washed and stained in 300 μl PBS containing 15 μl RNase A and 25 μl propidium iodide. After 1- h incubation away from light, cells were analyzed by flow cytometry using a FACSCalibur flow cytometer (BD Biosciences, San Jose, CA, USA). The percentage of the cells in each phase was analyzed using FlowJo software (San Carlos, CA USA).

Table 2. ASNS expression does not correlate with gender, tumor site and histology

Characteristics	*Total*	*Expression of ASNS*			P-*value*
		− *to* +	+	++	
Gender					
Male	20	0	8	12	0.268
Female	29	3	8	18	
Tumor site					
Right lung	27	1	9	17	0.736
Lift lung	22	2	7	13	
Histology					
Invasive adenocarcinoma	15	0	5	10	0.556
Micro-invasive adenocarcinoma	13	2	4	7	
Adenocarcinoma	21	1	7	13	
Tumor size (cm)					
<3	41	3	14	24	0.591
$\geqslant 3$	8	0	2	6	
Ki67 expression					
High	6	1	3	2	0.254
Low	43	2	13	28	

Statistical analysis

All statistical analyses were performed using SPSS13.0 software (SPSS Inc., Chicago, Illinois, USA). The differences between groups were analyzed by Student ferences between groupdemonstrated as mean ± SD of three independent experiments. Variables with a *P*-value <0.05 were considered statistically significant.

RESULTS

The expression of *ASNS* is increased in lung cancers

The data mining of microarray gene expression profiles by using Oncomine was carried out to investigate the expression level of *ASNS* mRNA in lung carcinoma tissues. It was found that expression of *ASNS* was elevated significantly in large cell lung carcinoma ($n=19$, $P=4.36E-9$) and squamous cell lung carcinoma ($n=27$, $P=1.67E-10$) as compared with normal lung tissues ($n=65$) by using the Hou Lung dataset, and was slightly upregulated in lung adenocarcinoma ($n=45$) (Figure 1a). Similarly, *ASNS* expression was significantly higher in lung adenocarcinoma ($n=86$, $P=2.10E-4$) than that in the normal tissues ($n=10$) as revealed in Beer Lung dataset (Figure 1b). In Selamat Lung dataset, *ASNS* expression was also increased in lung adenocarcinoma ($n=58$, $P=7.43E-13$) in comparison with the paired normal lung tissues ($n=58$) (Figure 1c). In addition, the above results were similar to another independent dataset, Stearman Lung, where *ASNS* was upregulated in lung adenocarcinoma ($n=20$, $P=2.38E-5$) as compared with the normal tissues (Figure 1d).

To confirm the above findings, we performed the IHC analysis of *ASNS* expression in lung adenocarcinoma tissues. As shown in Table 1, *ASNS* was significantly increased in tumor tissues ($n=49$, $P=0.003$) compared with that in the normal tissues ($n=13$). Representative images of IHC staining of the tumor tissues, the corresponding normal tissues and different intensities were shown in Figures 2a and b. Then, correlations between *ASNS* expression and clinicopathological factors in 49 lung cancer

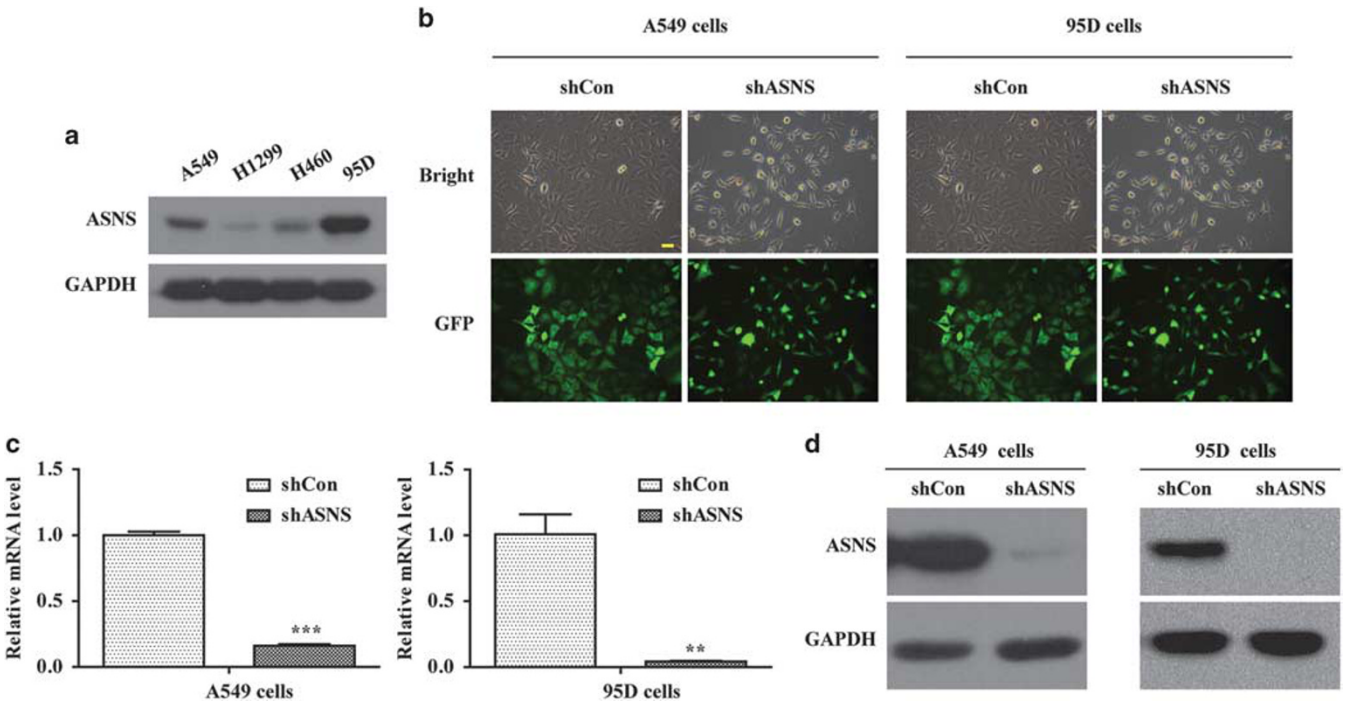

Figure 3. Knockdown efficiency of *ASNS* was shown in lung cancer cells. (**a**) Expression level of *ASNS* protein in human lung cancer cell lines was showed by the western blot analysis. (**b**) The representative images of successful lentivirus infection as indicated by green fluorescence in A549 and 95D cells. (**c**,**d**) Knockdown efficiency of *ASNS* in A549 and 95D cells was revealed by qRT-PCR and western blot assay, respectively. $^{**}P<0.01$, $^{***}P<0.001$, scales bar, 10 μm.

tissues were analyzed (Table 2). However, the expression rate of *ASNS* was not statistically associated with the gender ($P = 0.268$), tumor site ($P = 0.736$), histology ($P = 0.556$), tumor size ($P = 0.591$) or Ki67 expression ($P = 0.254$). Further studies on more clinical specimens are necessary to confirm the expression of *ASNS* as a potential diagnostic indicator in clinical lung cancer detection.

Silencing *ASNS* expression in human lung cancer cell lines

To clarify the role of *ASNS* in human lung cancer development *in vitro*, we first evaluated the expression level of *ASNS* in four lung cancer cell lines A549, H1299, H460 and 95D by western blot. As shown in Figure 3a, *ASNS* expression was observed in all these cell lines, and was highly expressed in A549 and 95D cell lines. Thus,

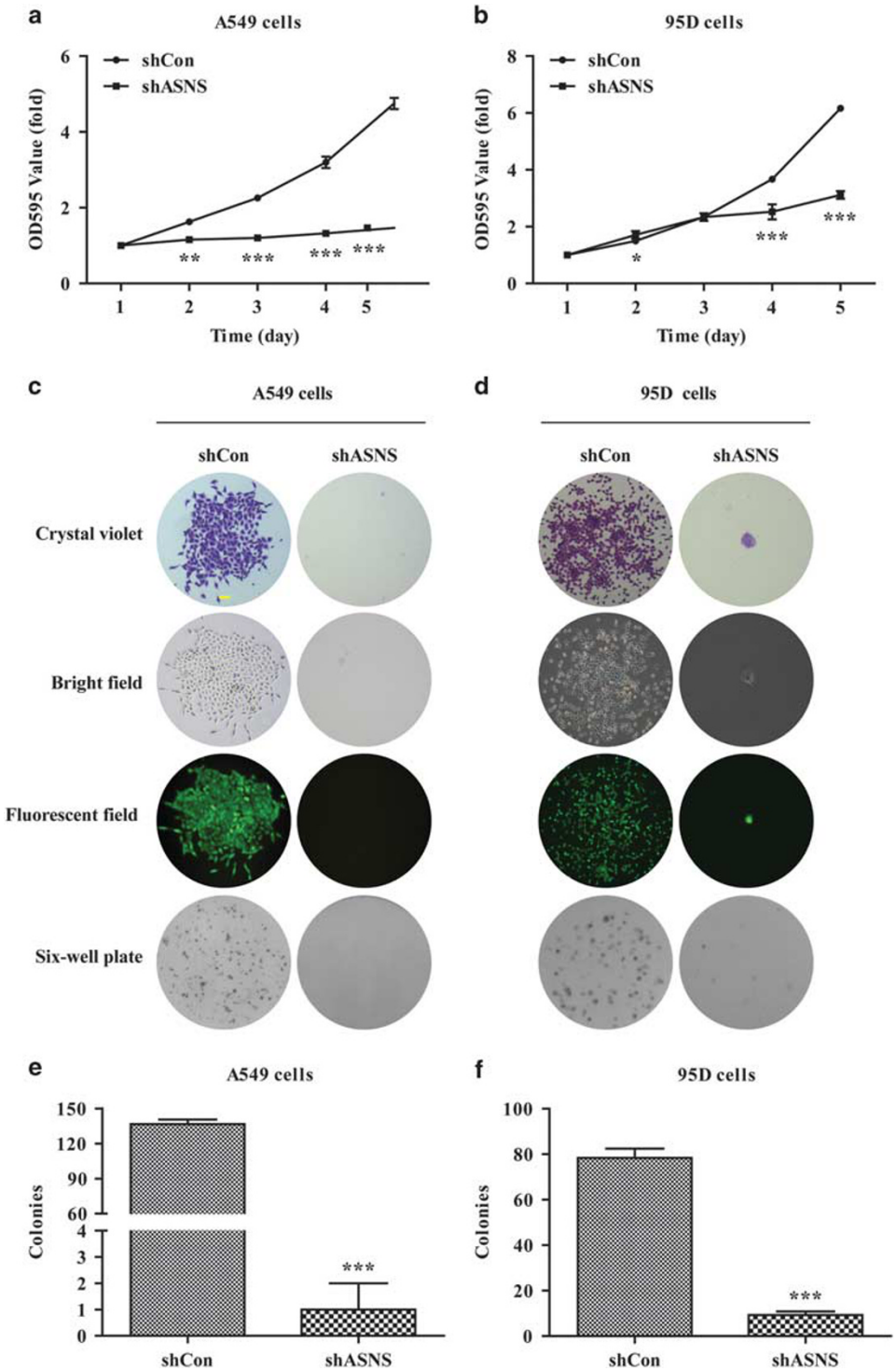

Figure 4. *ASNS* depletion suppressed the proliferation and colony formation of A549 and 95D cells. (**a**,**b**) The proliferation rate of A549 and 95D cells was significantly decreased after shASNS infection, respectively. (**c**,**d**) Representative images of single colony size and total numbers of colonies in A549 and 95D cells after shASNS infection were showed under microscopy. (**e**,**f**) Statistical analysis revealed the number of colonies in A549 and 95D cells. ***$P < 0.001$, scales bar, 25 μm.

we chose these two cell lines for further research *in vitro* by using RNA interference. Next, we silenced *ASNS* expression via lentivirus-mediated shRNA to assess the potential role of *ASNS* in regulating cell growth in A549 and 95D cells. Four days after lentivirus infection, the transfection efficiency was measured by assessing the expression of GFP. Figure 3b showed that the ratio of GFP-positive cells was over 90% in both A549 and 95D cells. Furthermore, *ASNS* knockdown efficiency was confirmed by qRT-PCR and western blot analysis. Compared with the control group (shCon), the expression level of *ASNS* mRNA in A549 and 95D cells in ASNS shRNA (shASNS) group significantly decreased by 83.9 and 95.7%, respectively (Figure 3c). Similarly, the intracellular protein level of *ASNS* in A549 and 95D cells was remarkably down-regulated in shASNS group (Figure 3d). These results demonstrated that the expression of *ASNS* was successfully silenced in A549 and 95D cells.

ASNS depletion inhibits the proliferation and colony formation of lung cancer cells

To determine the effect of *ASNS* depletion on lung cancer cell viability, MTT and colony formation assay were performed. As shown in Figures 4a and b, the growth rates of shASNS groups were significantly decreased by 69.1 and 49.4% in A549 and 95D cells compared to shCon groups on day 5 ($P < 0.001$). Moreover, both colony size and number of A549 and 95D cells in shASNS group were significantly decreased as compared with those in shCon group (Figures 4c and d). There were about 137 ± 4 colonies in shCon group vs 1 ± 1 colonies in shASNS group, indicating that the colony number decreased nearly by 99.3% in A549 cells ($P < 0.001$, Figure 4e). As shown in Figure 4f, the colony number of 95D cells reduced by approximately 88.1% in shASNS group as compared with that in shCon group (9 ± 2 vs 78 ± 4, $P < 0.001$). Taken together, the decreased expression of *ASNS* could diminish lung cancer cell proliferation and colony formation.

Knockdown of *ASNS* induces cell cycle arrest

Abnormal cell cycle is known as a common characteristic of human cancers. To investigate whether cell cycle arrest had a key role in cell growth inhibition, we analyzed the cell cycle distribution in A549 cells by flow cytometry (Figure 5a). In comparison with shCon group, knockdown of *ASNS* increased the percentage of G0/G1 phase cells in shASNS group ($78.37 \pm 0.57\%$ vs $69.80 \pm 0.60\%$, $P < 0.001$), decreased the percentage of in S phase ($16.63 \pm 0.70\%$ vs $20.98 \pm 0.160\%$, $P < 0.001$) and G2/M phase cells ($5.00 \pm 0.38\%$ vs $9.22 \pm 0.45\%$, $P < 0.001$, Figure 5b), suggesting that knockdown of *ASNS* could induce G0/G1 cell cycle arrest.

Knockdown of *ASNS* regulates the expression of cell cycle-related molecules

To further explore the mechanism underlying the inhibitory effect of *ASNS* knockdown on cell growth, the mRNA expression level of cell cycle regulators CDK2 and cyclin E1 was analyzed. As shown in Figure 5c, depletion of *ASNS* resulted in a significant decrease in the expression of CDK2 and cyclin E1 by qRT-PCR assay ($P < 0.05$),

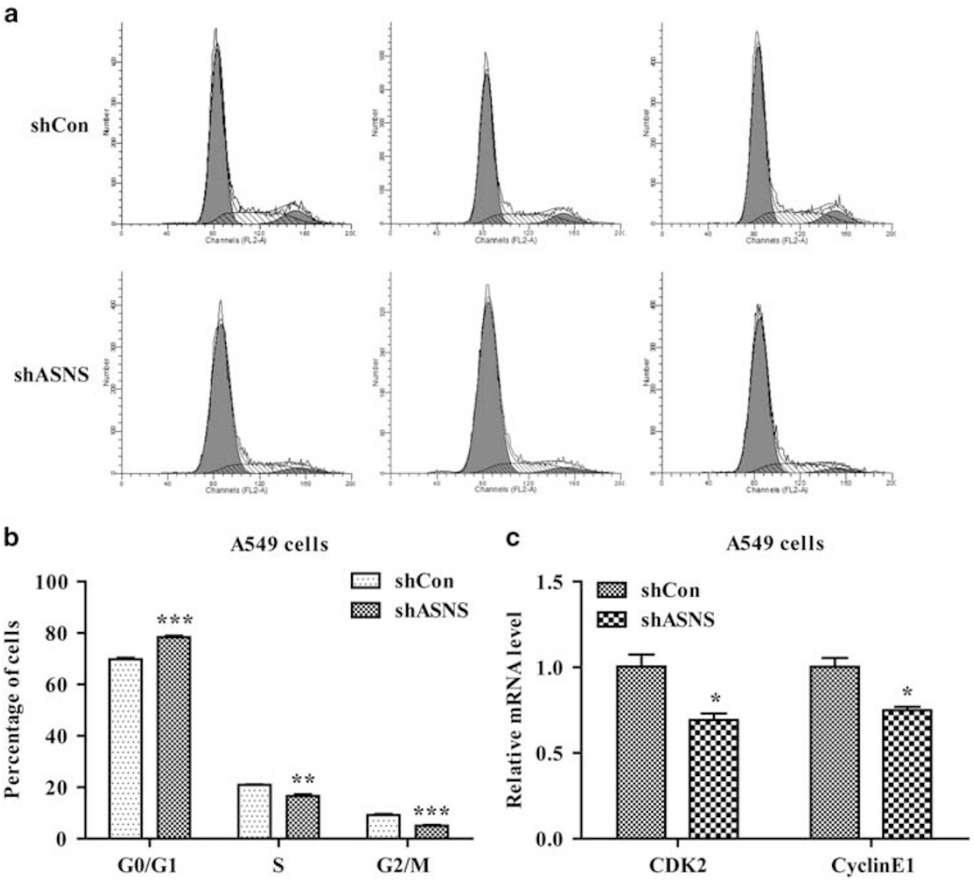

Figure 5. *ASNS* silencing arrested cell cycle progression in A549 cells. (**a**) Flow cytometry histograms were revealed the cell cycle progression of A549 cells in shCon and shASNS groups. (**b**) Statistical analysis revealed the percentage of cells in different phases of cell cycle. (**c**) The expression level of CDK2 and cyclin E1 mRNA in shCon and shASNS groups were analyzed by qRT-PCR. *$P < 0.05$, **$P < 0.01$, ***$P < 0.001$.

which may be the mechanism of how *ASNS* affected the development of lung cancer.

DISCUSSION

The potential biological function of *ASNS* in lung cancer remains elusive. It was found in the present study that *ASNS* was significantly upregulated in both lung cancer clinical tissues and cell lines. The result of the experiment with knocking down the *ASNS* expression showed that the expression of *ASNS* was closely associated with the occurrence and development of human lung cancer.

ASNS converses L-aspartate to L-asparagine, the abundance of amino acid, which always modulates serial fundamental progresses of gene expression, transcription factor recruitment, mRNA processing and translation.[18] Several studies[19–21] have illustrated that *ASNS* expression is linked to cell growth and its mRNA transcription is regulated by change in asparagine content. Asparagine could hydrolyze to aspartic acid by the catalysis of L-asparaginase, which has been applied in the treatment of acute lymphoblastic leukemia.[22] The curative effect of L-asparaginase leads to down-regulation of cellular asparagine and leukemic cells death.[23] Hutson *et al*.[6] found that the expression status of *ASNS* might be as a biomarker to detect the sensitivity to L-asparaginase in human leukemia cells. In addition, low expression of *ASNS* has been found to act as another target of L-asparaginase in some human solid cancer types such as pancreatic cancer,[24] ovarian cancer[8] and liver cancer.[10]

This is the first study reporting the potential role of *ASNS* in lung cancer. The results of IHC staining and Oncomine database mining of the present study showed that the expression levels of *ASNS* protein and mRNA were significantly upregulated in lung cancer tissues, which is consistent with the finding in castration-resistant prostate cancer.[11] Furthermore, we detected the inhibitory effect of *ASNS* depletion on the proliferation of lung cancer A549 and 95D cells in which *ASNS* was highly expressed *in vitro*. We found that *ASNS* silencing by small interfering RNA (siRNA) could inhibit the growth and proliferation of A549 and 95D cells markedly as shown by MTT and colony formation assay. Moreover, knockdown of *ASNS* induced cell cycle arrest at G0/G1 phase in A549 cells, which is also consistent with the previous finding that the growth of melanoma cells was arrested at G0/G1 phase after *ASNS* silencing.[25] Also, Basilico *et al*.[20,26] found that *ASNS* was essential for the progression of G1 phase and its deficiency could result in cell cycle arrest in hamster BHK cells. Above all, *ASNS* may prove to be a potential therapeutic target for lung cancer in future.

Extensive studies have demonstrated that CDKs and cyclins, two groups of important regulation molecules, could regulate the progression of cell cycle.[27–29] Cyclin E1 binding to CDK2 forms a specific complex of cyclin E1-CDK2, whose activity is necessary for cell cycle G1 to S phase transition.[30–32] It was found in this study that *ASNS* depletion suppressed the expression of CDK2 and cyclin E1, suggesting that *ASNS* silencing induced cell cycle arrest at G0/G1 phase potentially by inhibiting the formation of cyclin E1–CDK2 complex. Although the precise mechanism underlying this effect of *ASNS* on lung cancer cell growth needs to be further investigated, the result obtained in this study at least provides a primary notion for recognizing *ASNS* as a new target molecule that affects the development of human lung cancer.

In conclusion, our study demonstrated that *ASNS* had an important role in the growth of human lung cancer cells by inhibiting the proliferation and arresting cell cycle of lung cancer cells, suggesting *ASNS* may prove to be a potential therapeutic target for the pre-clinical and clinical researches of human lung cancer.

CONFLICT OF INTEREST

The authors declare no conflict of interest.

ACKNOWLEDGEMENTS

This work was supported by grants from the National Natural Science Foundation of China (No. 81572246).

REFERENCES

1 Siegel RL, Miller KD, Jemal A. Cancer statistics, 2015. *CA Cancer J Clin* 2015; **65**: 5–29.
2 Chen W, Zheng R, Baade PD, Zhang S, Zeng H, Bray F *et al.* Cancer statistics in China, 2015. *CA Cancer J Clin* 2016; **66**: 115–132.
3 Richards NG, Kilberg MS. Asparagine synthetase chemotherapy. *Annu Rev Biochem* 2006; **75**: 629–654.
4 Kilberg MS, Barbosa-Tessmann IP. Genomic sequences necessary for transcriptional activation by amino acid deprivation of mammalian cells. *J Nutr* 2002; **132**: 1801–1804.
5 Barbosa-Tessmann IP, Pineda VL, Nick HS, Schuster SM, Kilberg MS. Transcriptional regulation of the human asparagine synthetase gene by carbohydrate availability. *Biochem J* 1999; **339 (Pt 1):** 151–158.
6 Hutson RG, Kitoh T, Moraga Amador DA, Cosic S, Schuster SM, Kilberg MS. Amino acid control of asparagine synthetase: relation to asparaginase resistance in human leukemia cells. *Am J Physiol* 1997; **272**: C1691–C1699.
7 Cui H, Darmanin S, Natsuisaka M, Kondo T, Asaka M, Shindoh M *et al.* Enhanced expression of asparagine synthetase under glucose-deprived conditions protects pancreatic cancer cells from apoptosis induced by glucose deprivation and cisplatin. *Cancer Res* 2007; **67**: 3345–3355.
8 Lorenzi PL, Llamas J, Gunsior M, Ozbun L, Reinhold WC, Varma S *et al.* Asparagine synthetase is a predictive biomarker of L-asparaginase activity in ovarian cancer cell lines. *Mol Cancer Ther* 2008; **7**: 3123–3128.
9 Lorenzi PL, Reinhold WC, Rudelius M, Gunsior M, Shankavaram U, Bussey KJ *et al.* Asparagine synthetase as a causal, predictive biomarker for L-asparaginase activity in ovarian cancer cells. *Mol Cancer Ther* 2006; **5**: 2613–2623.
10 Zhang B, Dong LW, Tan YX, Zhang J, Pan YF, Yang C *et al.* Asparagine synthetase is an independent predictor of surgical survival and a potential therapeutic target in hepatocellular carcinoma. *Br J Cancer* 2013; **109**: 14–23.
11 Sircar K, Huang H, Hu L, Cogdell D, Dhillon J, Tzelepi V *et al.* Integrative molecular profiling reveals asparagine synthetase is a target in castration-resistant prostate cancer. *Am J Pathol* 2012; **180**: 895–903.
12 Beer DG, Kardia SL, Huang CC, Giordano TJ, Levin AM, Misek DE *et al.* Gene-expression profiles predict survival of patients with lung adenocarcinoma. *Nat Med* 2002; **8**: 816–824.
13 Hou J, Aerts J, den Hamer B, van Ijcken W, den Bakker M, Riegman P *et al.* Gene expression-based classification of non-small cell lung carcinomas and survival prediction. *PLoS ONE* 2010; **5**: e10312.
14 Selamat SA, Chung BS, Girard L, Zhang W, Zhang Y, Campan M *et al.* Genome-scale analysis of DNA methylation in lung adenocarcinoma and integration with mRNA expression. *Genome Res* 2012; **22**: 1197–1211.
15 Stearman RS, Dwyer-Nield L, Zerbe L, Blaine SA, Chan Z, Bunn PA Jr *et al.* Analysis of orthologous gene expression between human pulmonary adenocarcinoma and a carcinogen-induced murine model. *Am J Pathol* 2005; **167**: 1763–1775.
16 Wang J, Yu S, Cui L, Wang W, Li J, Wang K *et al.* Role of SMC1A overexpression as a predictor of poor prognosis in late stage colorectal cancer. *BMC Cancer* 2015; **15**: 90.
17 Zhou W, Wang Z, Shen N, Pi W, Jiang W, Huang J *et al.* Knockdown of ANLN by lentivirus inhibits cell growth and migration in human breast cancer. *Mol Cell Biochem* 2015; **398**: 11–19.
18 Kilberg MS, Pan YX, Chen H, Leung-Pineda V. Nutritional control of gene expression: how mammalian cells respond to amino acid limitation. *Annu Rev Nutr* 2005; **25**: 59–85.
19 Colletta G, Cirafici AM. TSH is able to induce cell cycle-related gene expression in rat thyroid cell. *Biochem Biophys Res Commun* 1992; **183**: 265–272.
20 Greco A, Ittmann M, Basilico C. Molecular cloning of a gene that is necessary for G1 progression in mammalian cells. *Proc Natl Acad Sci USA* 1987; **84**: 1565–1569.
21 Hongo S, Takeda M, Sato T. Induction of asparagine synthetase during lymphocyte activation by phytohemagglutinin. *Biochem Int* 1989; **18**: 661–666.
22 Verma N, Kumar K, Kaur G, Anand S. L-asparaginase: a promising chemotherapeutic agent. *Crit Rev Biotechnol* 2007; **27**: 45–62.
23 Appel IM, den Boer ML, Meijerink JP, Veerman AJ, Reniers NC, Pieters R. Up-regulation of asparagine synthetase expression is not linked to the clinical response L-asparaginase in pediatric acute lymphoblastic leukemia. *Blood* 2006; **107**: 4244–4249.

24 Dufour E, Gay F, Aguera K, Scoazec JY, Horand F, Lorenzi PL *et al*. Pancreatic tumor sensitivity to plasma L-asparagine starvation. *Pancreas* 2012; **41**: 940–948.
25 Li H, Zhou F, Du W, Dou J, Xu Y, Gao W *et al*. Knockdown of asparagine synthetase by RNAi suppresses cell growth in human melanoma cells and epidermoid carcinoma cells. *Biotechnol Appl Biochem* 2015; **63**: 328–333.
26 Gong SS, Basilico C. A mammalian temperature-sensitive mutation affecting G1 progression results from a single amino acid substitution in asparagine synthetase. *Nucleic Acids Res* 1990; **18**: 3509–3513.
27 Morgan DO. Principles of CDK regulation. *Nature* 1995; **374**: 131–134.
28 Weinberg RA. The retinoblastoma protein and cell cycle control. *Cell* 1995; **81**: 323–330.
29 Ekholm SV, Reed SI. Regulation of G(1) cyclin-dependent kinases in the mammalian cell cycle. *Curr Opin Cell Biol* 2000; **12**: 676–684.
30 Sherr CJ. G1 phase progression: cycling on cue. *Cell* 1994; **79**: 551–555.
31 Koff A, Giordano A, Desai D, Yamashita K, Harper JW, Elledge S *et al*. Formation and activation of a cyclin E-cdk2 complex during the G1 phase of the human cell cycle. *Science* 1992; **257**: 1689–1694.
32 Malumbres M, Barbacid M. Cell cycle kinases in cancer. *Curr Opin Genet Dev* 2007; **17**: 60–65.